Research Letter **DOI:** 10.15541/jim20240517

Low Temperature Sintering of $ZnAl_2O_4$ Ceramics with CuO-TiO_2-Nb_2O_5 Composite Oxide Sintering Aid

YANG Yan[1,2], ZHANG Faqiang[1], MA Mingsheng[1], WANG Yongzhe[1], OUYANG Qi[1], LIU Zhifu[1]

(1. CAS Key Lab of Inorganic Functional Materials and Devices, Shanghai Institute of Ceramics, Chinese Academy of Sciences, Shanghai 200050, China; 2. Technical Center, Yibin Red Star Electronics Co., Ltd., Yibin 644600, China)

Abstract: $ZnAl_2O_4$ and $ZnAl_2O_4$-based ceramics have attracted much attention from researchers due to their good microwave dielectric, thermal and mechanical properties. In this work, the influence of 5% (in mass) CuO-TiO_2-Nb_2O_5 (CTN) ternary composite oxide additives with different composition ratios on sintering behavior and properties of $ZnAl_2O_4$ microwave dielectric ceramics was investigated. When the molar fraction ranges of Cu, Ti and Nb elements in 5% CTN additives are 0.625–0.875, 0–0.250 and 0.125–0.625, respectively, sintering temperature of $ZnAl_2O_4$ ceramics can be reduced from above 1400 ℃ to below 1000 ℃. The sintering additives CN (Cu∶Nb=1∶1, molar ratio) and CTN (Cu∶Ti∶Nb=4∶1∶3, molar ratio) can reduce sintering temperature of $ZnAl_2O_4$ ceramics to 975 and 1000 ℃, respectively, while maintaining good dielectric properties (dielectric constant ε_r=11.36, quality factor $Q\times f$=8245 GHz and ε_r=9.52, $Q\times f$=22249 GHz) and flexural strengths (200 and 161 MPa), which are expected to be applied in preparation of low temperature co-fired ceramic (LTCC) materials with copper electrodes. Low-temperature sintering of the $ZnAl_2O_4$+CTN system is characterized as activated sintering. Nanometer-level amorphous interfacial films containing Cu, Ti, and Nb elements are observed at the grain boundaries, which may provide fast diffusion pathways for mass transportation during the sintering process. Valence changes of Ti and Cu ions, along with changes of oxygen vacancies, are confirmed, which provides a potential mechanism for reduced sintering temperature of $ZnAl_2O_4$ ceramics. In addition, a series of reactions occurring at the grain boundaries can activate these boundaries and further promote the sintering densification process. These results suggest a promising way to design a novel LTCC material with excellent properties based on the low temperature sintering of ceramics with the sintering aid of CuO-TiO_2-Nb_2O_5 composite oxide.

Key words: $ZnAl_2O_4$; CuO-TiO_2-Nb_2O_5; low-temperature sintering; microwave dielectric ceramic; low temperature co-fired ceramic

Multilayer co-fired ceramic substrates have extensive application in various electronic devices for miniaturization, high density, multi-function and high reliability. Based on the sintering temperature, these substrates can be divided into high temperature co-fired ceramic (HTCC) substrate and LTCC substrate. Alumina dielectrics combined with Mo and W conductors are typically selected for the HTCC material system, which are co-fired at temperatures exceeding 1500 ℃. HTCC substrate materials exhibit superior mechanical strength, high thermal conductivity and stable chemical performance. However, they also face challenges such as lower conductivity in Mo and W conductors and higher manufacturing costs. The conductors (Au, Ag, Cu, and alloys) with lower melting points and higher conductivity can be used in LTCC process (below 950 ℃), and thus LTCC has garnered significant scientific and commercial interest in recent years for the widespread applications in radio frequency components, integrated modules, packaging substrates and ceramic microsystems for high-speed and high-frequency communication[1-3]. To accommodate the low co-firing temperature of Au, Ag or

Received date: 2024-12-12; **Revised date:** 2025-02-19; **Published online:** 2025-02-25
Foundation item: National Natural Science Foundation of China (U24A2052); Shanghai Eastern Talent Plan
Biography: YANG Yan (1994–), female, PhD. E-mail: yan.yang@hongxing799.com
杨 燕(1994–), 女, 博士. E-mail: yan.yang@hongxing799.com
Corresponding author: LIU Zhifu, professor. E-mail: liuzf@mail.sic.ac.cn; MA Mingsheng, professor. E-mail: mamingsheng@mail.sic.ac.cn
刘志甫, 研究员. E-mail: liuzf@mail.sic.ac.cn; 马名生, 研究员. E-mail: mamingsheng@mail.sic.ac.cn

Cu conductors, various glass phases are commonly used to reduce the sintering temperature of LTCC materials[4-7]. However, the degradation of LTCC material properties due to the glass phase is inevitable[8]. For example, the thermal conductivity of commercial LTCC materials is constrained to 2–4 W/(m·K) due to the low thermal conductivity of the glass phase. Moreover, the brittle fracture of the glass phase leads to significantly reduced flexural strength compared to conventional ceramics, such as alumina and zirconia. Thus, there has been a sustained interest in developing high-performance LTCC materials without glass phase.

Researchers have done much work to reduce the sintering temperature of microwave dielectric ceramics by the implementation of composite oxides as additives instead of glass phases. Shigeno *et al*.[9-10] reported that Al_2O_3 ceramics can be sintered at 1000 ℃, achieving a high $Q\times f$ value of up to 23000 GHz, with a high thermal conductivity of 15 W/(m·K) and high mechanical strength of 450 MPa by adding CTN ternary oxide additives. Our previous work has further analyzed the low temperature sintering mechanism within Al_2O_3+CTN system[11]. The results revealed that the nanometer-thick amorphous films containing Cu, Ti and Nb formed on the grain boundaries, and the changes in the valence states of Cu and Ti ions were important for the low-temperature sintering of Al_2O_3 ceramics. In addition, the migration of Cu ions and associated reactions at the grain boundaries of Al_2O_3 ceramics could activate the grain boundaries and further promote the densification of Al_2O_3 ceramics. Based on these findings, the CTN could be expected to serve as the sintering aid to other oxide ceramic materials.

The $ZnAl_2O_4$ ceramics have excellent microwave dielectric properties (ε_r=8.5, $Q\times f$=56300 GHz, τ_f=–79×10^{-6} ℃$^{-1}$), good thermal conductivity of 20–25 W/(m·K), and a high flexural modulus of 242 GPa. However, the sintering temperature of $ZnAl_2O_4$ ceramics is typically above 1400 ℃[12-16]. Some efforts have been made to reduce the sintering temperature of $ZnAl_2O_4$ ceramics for LTCC application. Qin *et al*.[14] reported that the $ZnAl_2O_4$ ceramics could be sintered at 930 ℃ by adding Li-Mg-Zn-B-Si glass, yielding good microwave dielectric properties (ε_r~7.4, $Q\times f$~34100 GHz). Similarly, Thomas *et al*.[17] reported that the addition of $27B_2O_3$-$35Bi_2O_3$-$6SiO_2$-32ZnO glass could reduce the sintering temperature of $0.83ZnAl_2O_4$-$0.17TiO_2$ ceramics to 950 ℃, achieving $Q\times f$>10000 GHz, ε_r~10, and τ_f~–23×10^{-6} ℃$^{-1}$.

The feasibility of reducing the sintering temperature of $ZnAl_2O_4$ ceramic by adding CTN ternary oxide additives has been confirmed in our preliminary work[18]. Nevertheless, the optimal ratio of $CuO/TiO_2/Nb_2O_5$, as well as the sintering mechanism and resultant properties of $ZnAl_2O_4$ ceramics, are still unclear. To clarify the relationships among processing, microstructure, and property in the $ZnAl_2O_4$+CTN ceramics, the sintering behavior, microstructure, dielectric, thermal and mechanical properties of $ZnAl_2O_4$ ceramics were investigated systematically by adding CTN sintering aids with different $CuO/TiO_2/Nb_2O_5$ ratios in this work.

1 Experimental

The $ZnAl_2O_4$ ceramics with CTN sintering additives were prepared by conventional solid-state process. High purity (>99.99%) alumina powder (Shandong Sinocera Functional Material Co., Ltd., China), high purity (>99.9%) ZnO powder (Shanghai Macklin Biochemical Technology Co., Ltd., China), CuO, TiO_2 and Nb_2O_5 (Sinopharm Chemical Reagent Co., Ltd., China) were utilized as the starting materials. Stoichiometric amounts of ZnO and Al_2O_3 were mixed and ball-milled in ethanol for 6 h. The resulting slurry was then dried and calcined at 1150 ℃ for 4 h to form $ZnAl_2O_4$ phase. The obtained $ZnAl_2O_4$ powder was mixed with 5% (in mass) CTN additives with different composition ratios, followed by ball milling for 6 h in ethanol. The mixtures were dried, and subsequently mixed with 6% (in mass) polyvinyl alcohol (PVA) water solution as a binder. Cylinder, pellet, and long-bar shaped samples were fabricated using a compression machine for measurements of dielectric, thermal, and mechanical properties, respectively. The ceramic samples were obtained by sintering the green bodies in air at temperatures ranging from 900 ℃ to 1200 ℃ for 4 h, with a heating rate of 5 ℃/min. The sintered samples with different compositions of CTN additives were presented in supporting materials Fig. S1.

Density of the ceramic samples was determined by using Archimedes method. The microwave dielectric behaviors were measured at a frequency around 10 GHz by a network analyzer (E8363A, Agilent Technologies, USA). The dielectric constants (ε_r) and $Q\times f$ value were tested and calculated by Hakki-Coleman dielectric resonator method[19-20]. The coefficient of thermal expansion (CTE) was measured by a dilatometer (L75, Linseis, Germany) in the temperature range from 25 ℃ to 300 ℃. At least three samples were measured to determine the densities as well as dielectric and thermal properties, and the average data were taken as their corresponding properties. The flexural strength was evaluated using a three-point bending method in a universal testing machine (CTM2500, Xieqiang Instrument Manufacturing Co., Ltd., China).

Crystal phase identification was conducted *via* X-ray diffraction analysis (XRD, D8 Discover Davinci, Bruker

Axs Gmbh, Germany) in the 2θ range of 10º–80º. Microstructural images of the fracture surface of samples were obtained using a scanning electron microscope (SEM, SU8220, Hitachi, Japan). X-ray photoelectron spectroscopy (XPS, ESCALAB 250, Thermo Fisher Scientific, UK) was applied to analyze the valence states of elements. The grain boundary microstructures and elemental distribution analysis were observed by a transmission electron microscope (TEM, EM-2100F, JEOL, Japan) equipped with energy dispersion spectroscopy (EDS).

2 Results and discussion

The influence of CTN composition on the sintering behavior of alumina system has been reported[9]. However, the role of CTN additives in $ZnAl_2O_4$ system may not correspondingly align with that in Al_2O_3 system. The different compositions of CTN additives for $ZnAl_2O_4$, which were prepared in this work, are depicted in Fig. 1(a). The nephogram of sintering temperature for $ZnAl_2O_4$ ceramics with 5% CTN additives with different compositions is shown in Fig. 1(b). The data indicate that the sintering temperature of $ZnAl_2O_4$ ceramics could be tuned by altering the composition of CTN additives. Eight formulas of additives for $ZnAl_2O_4$ ceramics exhibit relatively low sintering temperatures below 1000 ℃, as highlighted in the blue region in Fig. 1(b). The compositions of CTN additives within this area corresponding to molar fraction ranges of Cu, Ti and Nb are 0.625–0.875, 0–0.250, and 0.125–0.625, respectively, while the sum of CuO, TiO_2 and $NbO_{2.5}$ molar fraction is 1. Notably, $ZnAl_2O_4$ ceramics demonstrate good densification at 1000 ℃ when the molar fractions of Cu, Ti and Nb are 0.500, 0.125 and 0.375, respectively. And the sintering temperature of $ZnAl_2O_4$ ceramics with the other seven additive formulas can be reduced to 975 ℃. When the composition of additives falls within the blue region, the well-sintered $ZnAl_2O_4$ ceramics show much darker colors than those outside this region, as shown in Fig. S1, which may be due to the significant presence of Cu element.

In order to clarify the role of Cu, Ti and Nb elements during the low temperature sintering process of $ZnAl_2O_4$ ceramics, nine formulas with different ratios of Cu : Ti : Nb and different sintering temperatures were selected as designated as the black points in Fig. 1(b). The molar fraction and corresponding sintering temperature are summarized in Table 1. Fig. 2 shows the XRD patterns of the sintered $ZnAl_2O_4$ ceramics with selected formulas of CTN additives. The main diffraction peaks are identified to be $ZnAl_2O_4$ (JCPDS: 05-0669). Notably, accompanied peaks of unknown new phases were observed in all samples except sample S4. It can't be concluded that there are no new phases formed in sample S4 due to the lower sensitivity of XRD for trace compounds. The chemical compositions of the unknown new phases are further discussed in the following EDS analysis. The new phases may play some beneficial roles in reducing the sintering temperature of ceramic matrix, as previously reported[11]. However, it is impossible to reduce the sintering temperature of $ZnAl_2O_4$ below 1000 ℃ with such minimal amounts of secondary phases, according to the conventional sintering mechanism.

To confirm the optimal formula, the density, dielectric, thermal and mechanical properties of $ZnAl_2O_4$ ceramics with nine different additives were measured, as shown in Table S1. The data in the table indicate that the dielectric constants of all sintered samples are significantly higher than those of pure $ZnAl_2O_4$ (ε_r~8.5) ceramics[9-10], which can be attributed to the presence of high dielectric constant oxides, such as TiO_2 and Nb_2O_5, in the CTN additives. And the samples S4 and S5 can strike a balance between good properties and lower sintering

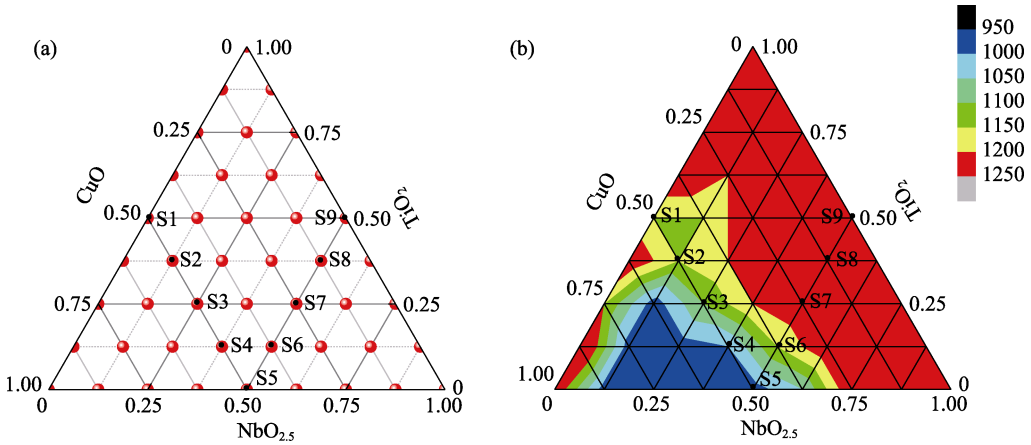

Fig. 1 (a) Compositions of CTN additives for $ZnAl_2O_4$; (b) Nephogram of sintering temperature of $ZnAl_2O_4$ ceramics with 5% CTN additives and different compositions

Colorful figures are available on website

Table 1 Sintering temperatures of $ZnAl_2O_4$ ceramics mixed 5% CTN additives with different formulas

Sample ID	Sintering temperature/℃	Molar fraction		
		Cu	Ti	Nb
S1	1150	0.500	0.500	0
S2	1150	0.500	0.375	0.125
S3	1100	0.500	0.250	0.250
S4	1000	0.500	0.125	0.375
S5	975	0.500	0	0.500
S6	1150	0.375	0.125	0.500
S7	1250	0.250	0.250	0.500
S8	1250	0.125	0.375	0.500
S9	1250	0	0.500	0.500

temperatures. Sample S4 can be sintered at 1000 ℃, demonstrating a high $Q\times f$ value of 22249 GHz, and a flexural strength of 161 MPa. For sample S5, the sintering temperature can be further reduced to 975 ℃, although its $Q\times f$ value decreases to 8245 GHz. However, the flexural strength of sample S5 increases to 200 MPa. The relatively lower flexural strength of sample S4, compared to sample S5, may be due to the larger grain size and the presence of more secondary phases, as illustrated in Fig. 3 and Fig. S2. In addition, the flexural strengths of the samples analyzed in this work surpass those of the majority of $ZnAl_2O_4$ microwave dielectric ceramics with glass phase additives (~140 MPa)[14], thereby highlighting the advantages of the glass-free additives. The CTE of the samples has no significant change, indicating that the addition of CTN has a limited effect on CTE.

Secondary electron SEM images of fracture surface of samples S4 and S5 sintered at 1000 and 975 ℃, respectively, were characterized as shown in Fig. 3. The dense microstructure is evident, which reveals that both samples are well sintered. The aggregation of the secondary phase occurs at certain triangular grain boundaries, as shown in Fig. S2. The average grain

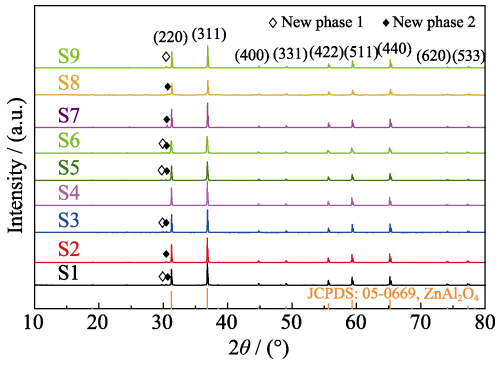

Fig. 2 XRD patterns of the sintered $ZnAl_2O_4$ ceramics mixed with 5% CTN additives according to different formulas

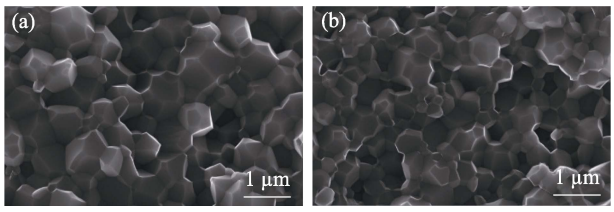

Fig. 3 Secondary electron SEM images of fracture surface of the sintered samples S4 (a) and S5 (b)

diameter, a characterization of grain size used in this work, is determined by the quotient of the diagonal length of sample and the number of grains in the diagonal portion based on Fig. S2. The average grain sizes of samples S4 and S5 are 0.5–0.6 and 0.4–0.5 μm, respectively. Sample S4 exhibits a larger grain size than sample S5, which may be due to the higher sintering temperature. It is noteworthy that no liquid phase was found in any of the samples. This is different from the formation of the liquid phase induced by CuO doping along the grain boundaries, which improves sinterability and promotes grain growth[21].

To further investigate the low temperature sintering behavior of the $ZnAl_2O_4$ ceramics with CTN, XPS characterizations of samples S4 and S5 were carried out. Fig. 4 shows the XPS spectra of sample S4. The fine scanning of each peak was performed to analyze the valence state of each element, with the results depicted in Fig. 4(b-e). The peak fitting curves of $Cu2p_{3/2}$ shown in Fig. 4(b) reveal two peaks with maximum binding energies at 932.6 and 933.7 eV, respectively, indicating the co-existence of Cu^+ and Cu^{2+} ions[22-23]. The content ratio of Cu^{2+} to Cu^+ is 0.7, as estimated from the integral peak areas of Cu^{2+} and Cu^+, respectively. In Fig. 4(c), the peaks with binding energies of 459.2 and 458.1 eV correspond to $Ti^{4+}2p_{3/2}$ and $Ti^{3+}2p_{3/2}$, respectively[24-27]. The content ratio of Ti^{4+} to Ti^{3+} is 1.8, based on the integral peak areas of these ions. These findings reveal that Cu^{2+}, Cu^+, Ti^{4+} and Ti^{3+} ions coexist in sample S4. During the process of high temperature sintering of the $ZnAl_2O_4$ ceramics, Cu^{2+} and Ti^{4+} ions can be partially reduced to Cu^+ and Ti^{3+}[28-30]. The valence changes of the active elements in the CTN additive may play an important role in the densification of $ZnAl_2O_4$ ceramics. The peaks with binding energy of 207.3 and 210.0 eV shown in Fig. 4(d) should correspond to $Nb3d_{5/2}$ and $Nb3d_{3/2}$ peaks of Nb^{5+}, respectively[31]. The peaks with binding energy of 530.0, 531.1 and 531.9 eV, as shown in Fig. 4(e), are identified as O1, O2 and O3, representing the lattice oxygen, defective oxygen and surface-adsorbed oxygen species, respectively[32-34].

The XPS spectra of sample S5 are shown in Fig. S3. Compared with Fig. 4(b), the relative content of Cu^{2+} in

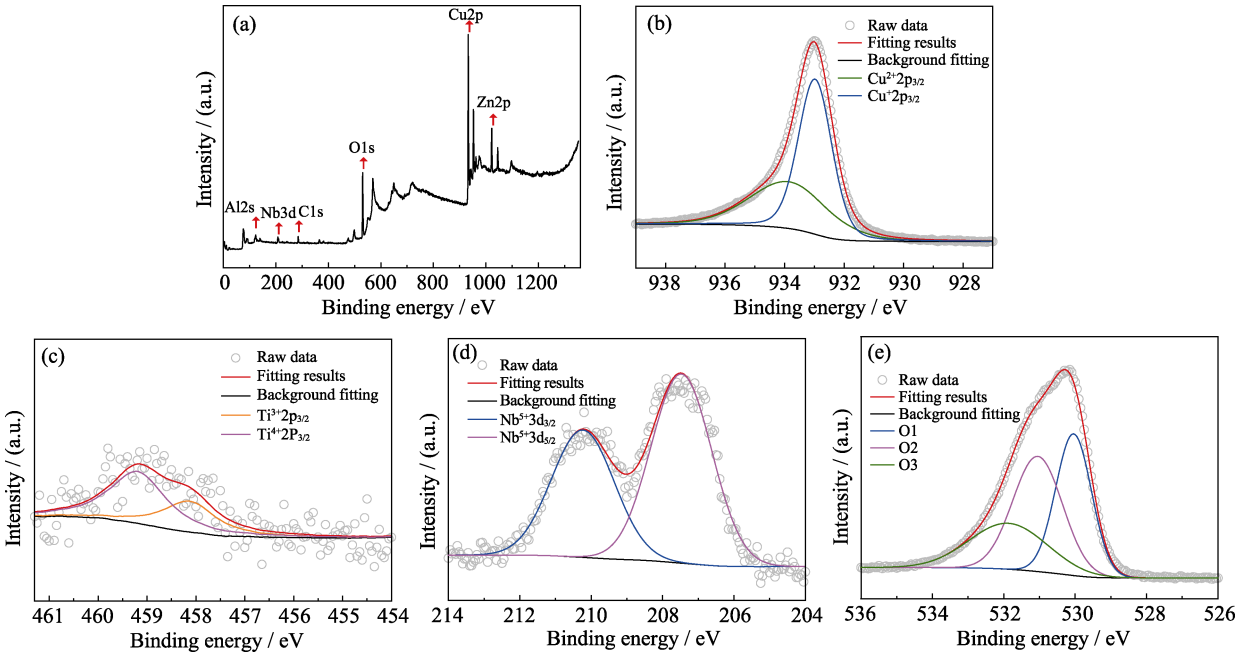

Fig. 4 XPS spectra of sample S4 sintered at 1000 ℃ for 2 h (a) and (b-e) detailed XPS spectra of Cu ion (b), Ti ion (c), Nb ion (d) and O1s (e)

Colorful figures are available on website

sample S5 is significantly higher than that in sample S4. This discrepancy is attributed to the limited oxygen on the sample surface being taken up by parts of Ti^{3+} to transform to Ti^{4+} during the cooling process of ceramic sintering, resulting in fewer available oxygen atoms for Cu^{+} to reform Cu^{2+}. In comparison with Fig. 4(e), the relative content of O2 in sample S5 is markedly higher than that in S4, indicating that the addition of Ti ions may introduce some oxygen and reduce the oxygen vacancy in $ZnAl_2O_4$ lattice[31], so that the extrinsic dielectric loss of sample S4 is diminished[35]. The promoting effect of defects on sintering is weakened with the reduction of oxygen vacancy, leading to a relatively higher sintering temperature.

In order to further understand the relationship between microstructures and properties of $ZnAl_2O_4$ ceramics with CTN additives, high resolution TEM (HRTEM) analysis was conducted to obtain a clearer image of the grain boundary. Fig. 5 shows the typical HRTEM images around the grain boundary of samples S4 and S5. An amorphous interfacial film with the thickness of about 2 nm is observed at the grain interface, which can be considered as a type of grain boundary complexion and promote rapid mass transport[36].

In order to analyze the element distribution, the corresponding EDS mappings of samples S4 and S5 were performed as shown in Fig. 6 and Fig. S4, respectively. The distribution of Ti element in sample S4 is not distinctly observable, which may be due to its low content. In contrast, Nb and Cu elements exhibit a preferential distribution at the grain boundaries of $ZnAl_2O_4$ ceramics, with an accumulation of Cu elements in the triangular grain boundary. It can be inferred that Cu elements could migrate from grain boundary to triangular grain boundary during the sintering process. This migration is related to the valence change of Cu between Cu^{2+} and Cu^{+}, which has been confirmed by XPS analysis.

The amorphous films and the defects formed during valence changing of Cu and Ti ions in the grain boundaries adversely affect the dielectric and mechanical properties of $ZnAl_2O_4$ ceramics, leading to reduced $Q\times f$ values and flexural strengths of samples S4 and S5. Nevertheless, the properties of the ceramics in this work

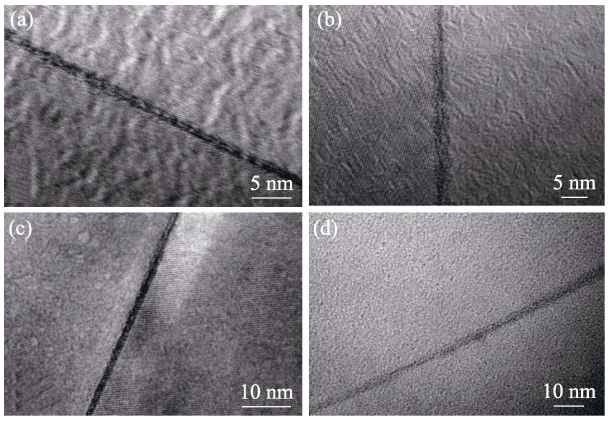

Fig. 5 HRTEM images of grain boundary complexion of sample S4 sintered at 1000 ℃ for 2 h (a, b) and sample S5 sintered at 975 ℃ for 2 h (c, d)

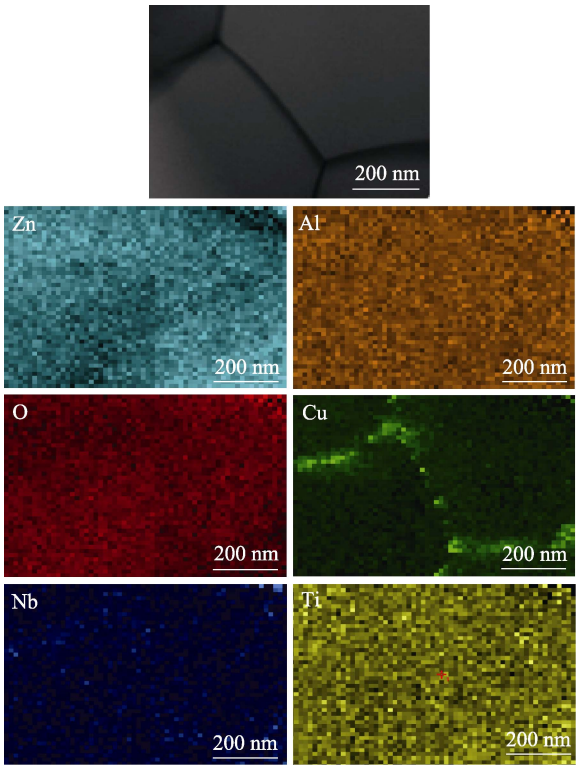

Fig. 6 EDS element mappings of sample S4 sintered at 1000 ℃ for 2 h

remain favorable for LTCC application, since the traditional LTCC materials with the addition of many glass phases exhibit lower $Q\times f$ values (≤3000 GHz) and flexural strengths (≤150 MPa).

According to the above analyses, there are some similar phenomena in low temperature sintered samples S4 and S5: (1) amorphous films with nanometer thickness were formed at grain boundaries of $ZnAl_2O_4$ ceramics; (2) Cu ions were likely to be enriched at triangular grain boundaries; (3) valence changes of Cu ions were observed during the sintering process. These phenomena might constitute key aspects of the low temperature sintering mechanism of $ZnAl_2O_4$ ceramics with CTN additives.

Surface diffusion, grain boundary diffusion, volume diffusion and evaporative condensation are considered the important mass transport mechanisms in ceramic sintering process, with grain boundary diffusion and volume diffusion predominating during the middle and final stages of sintering[37]. Given that the densification of samples S4 or S5 ceramic systems occurs at relatively low sintering temperatures, grain boundary transport is likely involved. Our previous work has demonstrated that the nanometer-thickness amorphous film at the grain boundary is considered as an interfacial complexion, which could be in a kind of quasi-liquid state under sintering conditions, thus serving as a short-circuit diffusion path for rapid mass transport[11]. The enhanced sintering facilitated by grain boundary complexion represents a form of activation sintering, wherein discrete nanoscale complexions act as activators[38-39]. In this work, the discrete nanoscale interfacial phase exists in an amorphous state and does not appear in bulk phase diagrams. And no liquid phase was detected in the SEM and TEM images. The amorphous films play an important role in reducing the sintering temperatures of samples S4 and S5 by providing the short-circuit diffusion path for rapid mass transport.

In addition, the valence changes of Cu ions could induce defects during their migration along the grain boundaries. The defects at grain boundaries, alongside the migration of Cu ions, would also contribute to the activation of grain boundaries and promote densification during the sintering process, resulting in the low sintering temperature of 1000 and 975 ℃ for samples S4 and S5, respectively. Furthermore, the addition of Ti ions may introduce some oxygen elements, thus reducing the oxygen vacancy in $ZnAl_2O_4$ lattice. The reduced defects would weaken the activated sintering of $ZnAl_2O_4$ ceramics, which makes the sample S4 have relatively higher sintering temperature.

3 Conclusions

The effects of CTN addition on sintering behavior and properties of $ZnAl_2O_4$ ceramics were studied systematically. The sintering temperature of $ZnAl_2O_4$ ceramics could be reduced to 975 ℃ by the addition of CTN, resulting in favorable dielectric properties (ε_r=11.36, $Q\times f$=8245 GHz) and a high flexural strength of 200 MPa. The amorphous film in the grain boundaries plays an important role in reducing the sintering temperature of $ZnAl_2O_4$ ceramics. However, the amorphous films, along with defects formed during valence changing of Cu and Ti ions within the grain boundaries, negatively impact the dielectric and mechanical properties of $ZnAl_2O_4$ ceramics. Nevertheless, the properties of the $ZnAl_2O_4$+CTN systems in this work are relatively improved compared with the previously reported works by the addition of glass phases to $ZnAl_2O_4$ ceramics. This work provides a feasible way for designing new LTCC materials without glass addition.

Supporting Materials

Supporting materials related to this article can be found at https://doi.org/10.15541/jim20240517.

References:

[1] NAGATSUMA T, DUCOURNAU G, RENAUD C C. Advances in

terahertz communications accelerated by photonics. *Nature Photonics*, 2016, **10:** 371.

[2] MA M S, WANG Y, NAVARRO-CÍA M, *et al*. The dielectric properties of some ceramic substrate materials at terahertz frequencies. *Journal of the European Ceramic Society*, 2019, **39:** 4424.

[3] TAJIMA T, SONG H J, YAITA M. Compact THz LTCC receiver module for 300 GHz wireless communications. *IEEE Microwave and Wireless Components Letters*, 2016, **26:** 291.

[4] CHEN X, ZHANG W, BAI S, *et al*. Densification and characterization of SiO_2-B_2O_3-CaO-MgO glass/Al_2O_3 composites for LTCC application. *Ceramics International*, 2013, **39:** 6355.

[5] ARCARO S, CESCONETO FR, PEREIRA F R, *et al*. Synthesis and characterization of LZS/A-Al_2O_3 glass-ceramic composites for applications in the LTCC technology. *Ceramics International*, 2014, **40:** 5269.

[6] SEBASTIAN M T, JANTUNEN H. Low loss dielectric materials for LTCC applications: a review. *International Materials Reviews*, 2008, **53:** 57.

[7] ZHOU J. Towards rational design of low-temperature co-fired ceramic (LTCC) materials. *Journal of Advanced Ceramics*, 2012, **1:** 89.

[8] RABE T, GEMEINERT M, SCHILLER W A. Development of advanced low temperature cofired ceramics (LTCC). *Key Engineering Materials*, 2004, **264–268:** 1181.

[9] SHIGENO K, KATSUMURA H, KAGATA H, *et al*. Low temperature sintering of alumina by CuO-TiO_2-Nb_2O_5 additives. *Key Engineering Materials*, 2006, **320:** 181.

[10] SHIGENO K, KOJIMA E, FUJIMORI H. Improvement in the low-temperature sintering performance and characteristics of alumina with CuO-TiO_2-Nb_2O_5 additive by controlling the firing atmosphere. *Journal of the Japan Society of Powder and Powder Metallurgy*, 2016, **63:** 701.

[11] YANG Y, MA M S, ZHANG F Q, *et al*. Low-temperature sintering of Al_2O_3 ceramics doped with $4CuO$-TiO_2-$2Nb_2O_5$ composite oxide sintering aid. *Journal of the European Ceramic Society,* 2020, **40:** 5504.

[12] LEI W, LU W Z, ZHU J H, *et al*. Microwave dielectric properties of $ZnAl_2O_4$-TiO_2 spinel-based composites. *Materials Letters*, 2007, **61:** 4066.

[13] SURENDRAN K P, SANTHA N, MOHANAN P, *et al*. Temperature stable low loss ceramic dielectrics in $(1–x)ZnAl_2O_4–xTiO_2$ system for microwave substrate applications. *European Physical Journal B*, 2004, **41:** 301.

[14] QIN T Y, ZHONG C W, QIN Y, *et al*. Low-temperature sintering mechanism and microwave dielectric properties of $ZnAl_2O_4$-LMZBS composites. *Journal of Alloys and Compounds*, 2019, **797:** 744.

[15] ROSHNI S B, SEBASTIAN M T, SURENDRAN K P. Can zinc aluminate-titania composite be an alternative for alumina as microelectronic substrate? *Scientific Reports*, 2017, **7:** 40839.

[16] WU J M, LU W Z, LEI W, *et al*. Preparation of $ZnAl_2O_4$-based microwave dielectric ceramics and GPS antenna by aqueous gel casting. *Materials Research Bulletin*, 2011, **46:** 1485.

[17] THOMAS S, SEBASTIAN M T. Effect of B_2O_3-Bi_2O_3-SiO_2-ZnO glass on the sintering and microwave dielectric properties of $0.83ZnAl_2O_4$-$0.17TiO_2$. *Materials Research Bulletin*, 2008, **43:** 843.

[18] YANG Y, MA M S, WANG Y Z, *et al*. Low-temperature sintering of $ZnAl_2O_4$ ceramics with $4CuO$-TiO_2-$2Nb_2O_5$ composite oxide sintering aid. *Ferroelectrics*, 2022, **586:** 190.

[19] COURTNEY W E. Analysis and evaluation of a method of measuring the complex permittivity and permeability microwave insulators. *IEEE Transaction on Microwave Theory and Techniques*, 1970, **18:** 476.

[20] HAKKI B W, COLEMAN P D. A dielectric resonator method of measuring inductive capacitance in the millimeter range. *IEEE Transaction on Microwave Theory and Techniques*, 1960, **8:** 402.

[21] DIFEO M, RAMAJO L, CASTRO M. Influence of CuO addition on dielectric and piezoelectric properties of $(Bi_{0.5}Na_{0.5})$ TiO_3-$BaTiO_3$ lead-free piezoceramics. *Journal of Advanced Dielectrics*, 2021, **11:** 2140004.

[22] MCLNTYRE N S, COOK M G. X-ray photoelectron studies on some oxides and hydroxides of cobalt, nickel, and copper. *Analytical Chemistry*, 1975, **47:** 2208.

[23] SUZANA M, FRANCISCO P, MASTERARO V R. Activity and characterization by XPS, HRTEM, Raman spectroscopy, and BET surface area of CuO/CeO_2-TiO_2 catalysts. *The Journal of Physical Chemistry B*, 2001, **105:** 10515.

[24] SANJINÉS R, TANG H, BERGER H, *et al*. Electronic structure of anatase TiO_2 oxide. *Journal of Applied Physiology*, 1994, **75:** 2945.

[25] MOREAU P, OUVRARD G, GRESSIER P, *et al*. Electronic structures and charge transfer in lithium and mercury intercalated titanium disulfides. *Journal of Physics and Chemistry of Solids*, 1996, **57:** 1117.

[26] UEKAWA N, WATANABE M, KANEKO K. Mixed-valence formation in highly oriented Ti-doped iron oxide film. *Journal of the Chemical Society, Faraday Transaction*, 1995, **91:** 2161.

[27] WERFEL F, BRUMMER O. Corundum structure oxides studied by XPS. *Physical Scripta*, 1983, **28:** 92.

[28] LU F H, FANG F X, CHEN Y S. Eutectic reaction between copper oxide and titanium dioxide. *Journal of the European Ceramic Society*, 2001, **21:** 1093.

[29] YOSHIDA H, YAMAMOTO T. Densification behavior of Ti-doped polycrystalline alumina in a nitrogen-hydrogen atmosphere. *Materials Transactions*, 2009, **50:** 1032.

[30] PULLAR R C, PENN S J, WANG X, *et al*. Dielectric loss caused by oxygen vacancies in titania ceramics. *Journal of the European Ceramic Society*, 2009, **29:** 419.

[31] POLLAK R A, STOLZ H J, RAIDER S I, *et al*. Chemical composition and interface chemistry of very thin Nb_2O_5 films prepared by RF plasma oxidation. *Oxidation of Metals*, 1983, **20:** 185.

[32] OU G, XU YS, WEN B, *et al*. Tuning defects in oxides at room temperature by lithium reduction. *Nature Communications*, 2018, **9:** 1302.

[33] CHEN, X B, LIU L, YU P Y, *et al*. Increasing solar absorption for photocatalysis with black hydrogenated titanium dioxide nanocrystals. *Science*, 2011, **331:** 746.

[34] HU W B, LIU Y, WITHERS R L, *et al*. Electron-pinned defect-dipoles for high-performance colossal permittivity materials. *Nature Materials*, 2013, **12:** 821.

[35] THIRUMAL M, MURUGAN G S, VARMA K B R, *et al*. $Ba_3ZnTa_{2-x}Nb_xO_9$ and $Ba_3MgTa_{2-x}Nb_xO_9$: synthesis, structural and dielectric studies. *Materials Research Bulletin*, 2000, **35:** 2423.

[36] NIE J Y, CHAN J M, QIN M D, *et al*. Liquid-like grain boundary complexion and sub-eutectic activated sintering in CuO-doped TiO_2. *Acta Materials*, 2017, **130:** 329.

[37] KINGERY W D, BOWEN H K, UHLMANN D R. Introduction to Ceramics, 2nd edition. New York: John Wiley and Sons, 1976: 478–482.

[38] GUPTA V K, YOON D H, MEYER H M, *et al*. Thin intergranular films and solid state activated sintering in nickel- doped tungsten. *Acta Materials*, 2007, **55:** 3131.

[39] LUO J, WANG H, CHIANG Y M. Origin of solid-state activated sintering in Bi_2O_3-doped ZnO. *Journal of the American Ceramic Society*, 1999, **82:** 916.

基于 $CuO\text{-}TiO_2\text{-}Nb_2O_5$ 复合氧化物烧结助剂的 $ZnAl_2O_4$ 陶瓷低温烧结研究

杨 燕[1,2], 张发强[1], 马名生[1], 王墉哲[1], 欧阳琪[1], 刘志甫[1]

(1. 中国科学院 上海硅酸盐研究所, 无机功能材料与器件重点实验室, 上海 200050; 2. 宜宾红星电子有限公司技术中心, 宜宾 644600)

摘 要: $ZnAl_2O_4$ 及 $ZnAl_2O_4$ 基陶瓷由于具有优良的微波介电、热学和力学性能, 从而备受研究人员关注。本工作系统研究了不同组成比例的 5% $CuO\text{-}TiO_2\text{-}Nb_2O_5$(CTN)三元复合氧化物烧结助剂对 $ZnAl_2O_4$ 微波介电陶瓷烧结行为和性能的影响。当 5% CTN 烧结助剂中 Cu、Ti、Nb 元素的摩尔分数分别为 0.625~0.875、0~0.250、0.125~0.625 时, $ZnAl_2O_4$ 陶瓷的烧结温度可从 1400 ℃以上降低至 1000 ℃以下。烧结助剂 CN(Cu∶Nb=1∶1, 摩尔比)和 CTN(Cu∶Ti∶Nb=4∶1∶3, 摩尔比)可分别将 $ZnAl_2O_4$ 陶瓷的烧结温度降低至 975 和 1000 ℃, 同时陶瓷具有优良的介电性能(介电常数 ε_r=11.36, 品质因数 $Q\times f$=8245 GHz; ε_r=9.52, $Q\times f$=22249 GHz)和抗弯强度(200 和 161 MPa), 有望用于制备铜电极低温共烧陶瓷(LTCC)材料。$ZnAl_2O_4$+CTN 体系的低温烧结是一种活化烧结机制。晶界处存在含 Cu、Ti、Nb 元素的纳米级非晶态界面膜, 在 $ZnAl_2O_4$ 陶瓷烧结过程中为传质过程提供了快速扩散路径。Ti 和 Cu 离子的化合价改变以及氧空位变化, 降低了 $ZnAl_2O_4$ 陶瓷的烧结温度。此外, 晶界上发生的系列反应发挥了活化晶界的作用, 进一步促进烧结致密化。本工作为设计具有优良性能、$CuO\text{-}TiO_2\text{-}Nb_2O_5$ 复合氧化物助烧的 $ZnAl_2O_4$ 陶瓷 LTCC 材料提供了一种参考。

关 键 词: $ZnAl_2O_4$; $CuO\text{-}TiO_2\text{-}Nb_2O_5$; 低温烧结; 微波介质陶瓷; 低温共烧陶瓷

中图分类号: TM282 **文献标志码:** A **文章编号:** 1000-324X(2025)06-0711-08

Supporting Materials:

Low Temperature Sintering of $ZnAl_2O_4$ Ceramics with CuO-TiO_2-Nb_2O_5 Composite Oxide Sintering Aid

YANG Yan[1,2], ZHANG Faqiang[1], MA Mingsheng[1], WANG Yongzhe[1], OUYANG Qi[1], LIU Zhifu[1]

(1. CAS Key Lab of Inorganic Functional Materials and Devices, Shanghai Institute of Ceramics, Chinese Academy of Sciences, Shanghai 200050, China; 2. Technical Center, Yibin Red Star Electronics Co., Ltd., Yibin 644600, China)

S1 Camera images of the sintered samples with different compositions of CTN additives

The well densified $ZnAl_2O_4$ ceramics with 5% (in mass) CTN additives of different compositions show dark colors when the molar fraction ranges of Cu, Ti, Nb are 0.625–0.875, 0–0.250, and 0.125–0.625, respectively. It may be contributed to the large amount of Cu element, which is sensitive to oxygen partial pressure and could improve the sintering process of $ZnAl_2O_4$ ceramics as discussed in Fig. 3-Fig. 6.

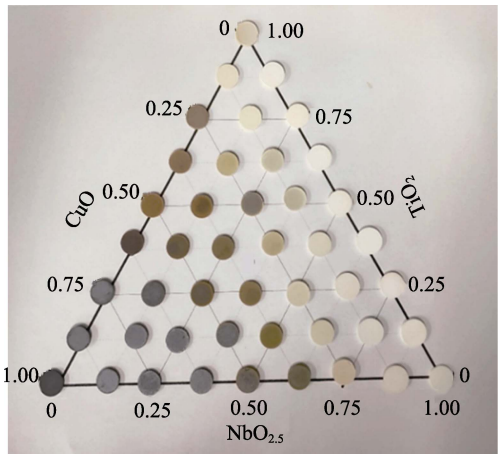

Fig. S1 Camera images of the sintered samples with different compositions of CTN additives

S2 Properties of $ZnAl_2O_4$ ceramics with different formulas of CTN additives

To confirm the optimal formula, the density, dielectric, thermal and mechanical properties of $ZnAl_2O_4$ ceramics with nine different additives were measured, as shown in Table S1. The dielectric constants of all sintered samples are higher than that of pure $ZnAl_2O_4$ (ε_r~8.5) ceramics, because there are oxides like TiO_2 and Nb_2O_5 with high dielectric constant in the CTN additives. Since samples S7, S8 and S9 present low density at the sintering temperature of 1250 ℃, the dielectric properties of them cannot be obtained by the Hakki-Coleman measurement method. Sample S4 can be sintered at 1000 ℃ and possesses a high $Q\times f$ value of 22249 GHz and a high density of 4.54 g/cm^3. For sample S5, the sintering temperature can be further reduced to 975 ℃, but the $Q\times f$ value reduced to 8245 GHz. While, the flexural strength of sample S5 increased to 200 MPa. The higher flexural strength of above 230 MPa can also be obtained from samples S1, S2 and S3, but the corresponding sintering temperature of them is above 1100 ℃. It suggests that samples S4 and S5 can strike a balance between good properties and lower sintering temperatures. Sample S4 has a lower flexural strength than that of sample S5, which may be due to the influence of larger grain and more secondary phases (as shown in Fig. 3). The coefficient of thermal expansion (CTE) of the samples has no significant

Table S1 Properties of $ZnAl_2O_4$ ceramics with different formulas of CTN additives

Sample ID	Sintering temperature/℃	Density/(g·cm^{-3})	ε_r(@10 GHz)	$Q\times f$/GHz	CTE/(×10^{-6}, ℃$^{-1}$) (25–350 ℃)	Flexural strength/MPa
S1	1150	4.46±0.17	10.18	17811	7.66	246±34
S2	1150	4.49±0.02	9.00	41673	7.34	230±10
S3	1100	4.49±0.01	10.10	17150	7.65	233±10
S4	1000	4.54±0.03	9.52	22249	7.49	161±25
S5	975	4.50±0.04	11.36	8245	7.56	200±14
S6	1150	4.54±0.01	9.67	30021	7.45	186±10
S7	1250	4.17±0.02	–	–	7.47	215±20
S8	1250	4.19±0.02	–	–	7.53	199±8
S9	1250	3.51±0.03	–	–	7.29	195±17

change, indicating that the addition of CTN has limited effect on CTE.

S3 Backscattered electron SEM images of the fracture surface of the sintered samples

Dense microstructure and regular crystallographic plane of grains could be observed, which reveals that these two samples have been well sintered. The aggregation of the second phase occurs at some triangular grain boundaries. Very thin grain boundary layer between grains can be seen from the backscattered electron SEM images shown in Fig. S2. Relatively weak grain boundary layers resulted in the intergranular fracture of the ceramics (as shown in Fig. 3 in the manuscript). The very bright contrast at the triple junctions of grains should be caused by the accumulation of CTN or CN, which is confirmed by the following TEM and EDS analysis. There is no liquid found in both samples. The average grain sizes of sample S4 and S5 are about 0.5–0.6 μm and 0.4–0.5 μm, respectively. Sample S4 shows larger grain size than that of sample S5 because of the higher sintering temperature of S4.

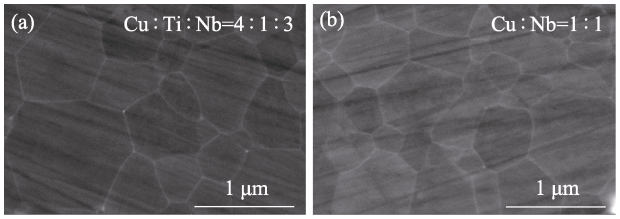

Fig. S2 Backscattered electron SEM images of the fracture surface of samples S4 and S5

S4 XPS spectra of S5 ceramic sintered at 1000 ℃ for 2 h

The XPS spectra of sample S5 are shown in Fig. S3. Full spectrum shown in Fig. S3(a) present the peaks of Al2s, Nb3d, Zn2p, O1s, Cu2p and C1s. The peak fitting curve of $Cu2p_{3/2}$ shown in Fig. S3(b) has two peaks with maximums at 932.9 and 934.4 eV, respectively, which indicates the coexistence of Cu^{+} and Cu^{2+}. As discussed in the manuscript, Cu^{2+} ions could be partially reduced to Cu^{+} during the sintering process. Compared with Fig. 4(b), the relative contents of Cu^{2+} in sample S5 is much higher than that in sample S4, because parts of the limited oxygen on the sample surface is taken up by parts of Ti^{3+} to transform to Ti^{4+} during the cooling process of ceramic sintering, and thus causing less oxygen for Cu^{+} to reform Cu^{2+}.The peaks for the Nb^{5+}, O1 and O3 are shown in Fig. S3(c, d). Compared with Fig. 4(e), the relative content of O2 in sample S5 is significantly higher than that of in S4, indicating that the addition of Ti ions may introduce some oxygen and reduce the oxygen vacancy in $ZnAl_2O_4$ lattice, so that the extrinsic dielectric loss of sample S4 decreased. The promoting effect of defects on sintering is weakened with the

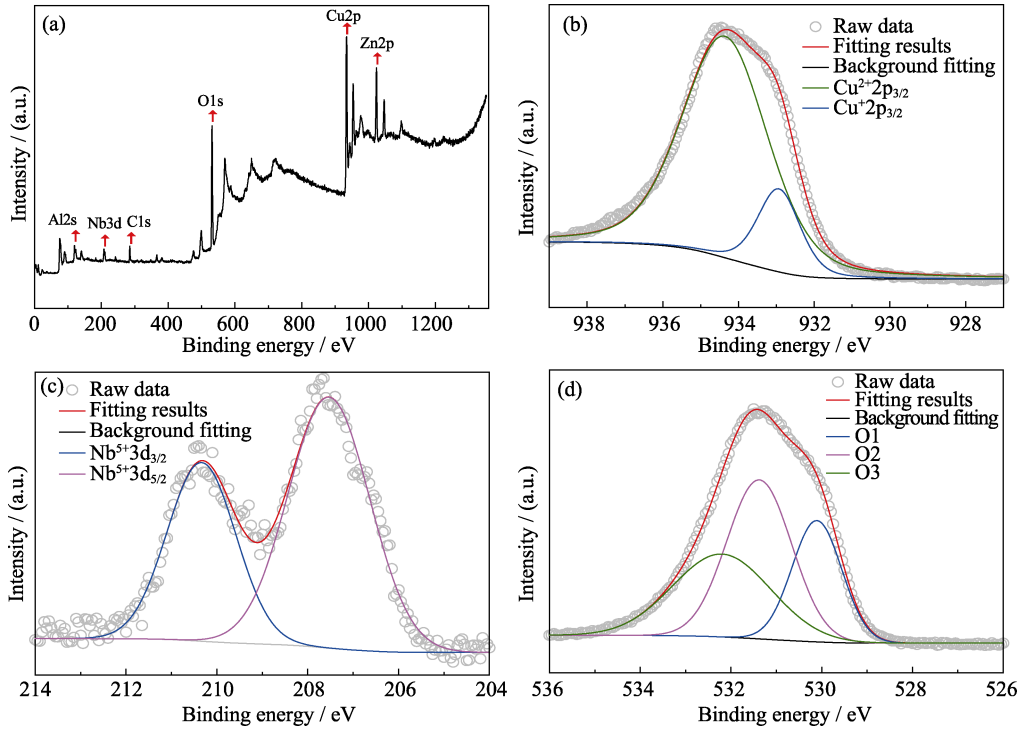

Fig. S3 XPS spectra of sample S5 sintered at 1000 ℃ for 2 h (a) and detailed XPS spectra of Cu ion (b), Nb ion (c) and O1s (d)

reduction of oxygen vacancy, which makes it have relatively higher sintering temperature.

S5 Valence change of Cu^{2+} and Ti^{4+} ions during the high temperature sintering process of the $ZnAl_2O_4$ ceramics

Cu^{2+} and Ti^{4+} ions are considered to be very sensitive to oxygen partial pressure at high temperatures. Cu^{2+} and Ti^{4+} ions can be partially reduced to Cu^{+} and Ti^{3+} by the following reactions in an anoxic environment, during the process of high temperature sintering of the $ZnAl_2O_4$ ceramics:

$$O_O^{\times} \leftrightharpoons \frac{1}{2}O_2 + V_{\ddot{O}} + 2e' \quad (S1)$$

$$Ti^{4+} + e' \leftrightharpoons Ti^{3+} \quad (S2)$$

$$Cu^{2+} + e' \leftrightharpoons Cu^{+} \quad (S3)$$

S6 EDS element mappings of sample S5 sintered at 975 ℃ for 2 h and EDS spectra of grain phase and the adjacent second phase

There was also an accumulation of Cu elements in the grain boundary triple junction as shown in Fig. S4(a). And the second phase was found where Cu and Nb elements were mainly distributed. The EDS analysis was carried out to get the element contents of the grain (marked as Area 1 in Fig. S4(a)) and second phase (marked as Area 2), and the results were shown in Fig. S4(b) and Table S2. Zn and Al elements were mainly distributed in the grains with little Cu elements. The molar ratio of Zn : Al is close to 1 : 2, which revealed that the main phase of Area 1 should be $ZnAl_2O_4$. Zn, Al, Cu and Nb elements were all found in Area 2. It suggests that there may be the crystallized $ZnAl_2O_4$ and some other oxides containing Zn-Nb-Cu-O elements.

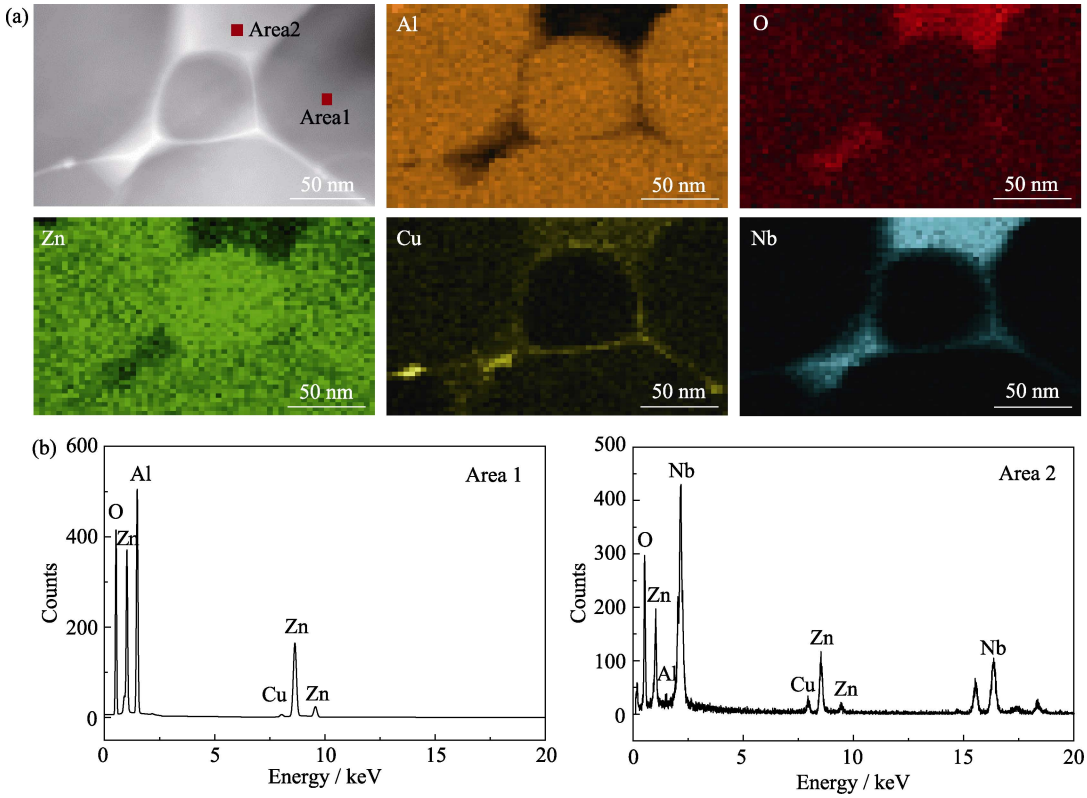

Fig. S4 EDS element mappings of sample S5 sintered at 975 ℃ for 2 h (a) and EDS spectra of the grain phase (Area 1) and the adjacent second phase (Area 2) (b)

Table S2 EDS analysis results for the grain (Area 1) and the adjacent second phase (Area 2)

Element		Al (K)	Zn(K)	O (K)	Nb (K)	Cu (K)
Atomic/%	Area 1	28.63	13.50	57.47	0.00	0.38
	Area 2	1.44	4.43	88.90	4.04	1.17
Uncertainty/%	Area 1	0.31	0.42	0.49	100.00	0.05
	Area 2	0.11	0.43	1.14	0.78	0.19